High-Pressure Rheology and Viscoelastic Scaling Predictions of Polymer Melts Containing Liquid and Supercritical Carbon Dioxide

JOSEPH R. ROYER,[1] JOSEPH M. DESIMONE,[1,2] SAAD A. KHAN[1]

[1]Department of Chemical Engineering, North Carolina State University, Raleigh, North Carolina 27695

[2]Department of Chemistry, University of North Carolina, Chapel Hill, North Carolina 27599

Received 23 October 2000; revised 17 September 2001; accepted 17 September 2001

ABSTRACT: High-pressure rheological behavior of polymer melts containing dissolved carbon dioxide (CO_2) at concentrations up to 6 wt % were investigated using a high-pressure extrusion slit die rheometer. In particular, the steady shear viscosity of poly(methyl methacrylate), polypropylene, low-density polyethylene, and poly(vinylidene fluoride) with dissolved CO_2 were measured for shear rates ranging from 1 to 500 s^{-1} and under pressure conditions up to 30 MPa. The viscosity of all samples revealed a reduction in the presence of CO_2 with its extent dependent on CO_2 concentration, pressure, and the polymer used. Two types of viscoelastic scaling models were developed to predict the effects of both CO_2 concentration and pressure on the viscosity of the polymer melts. The first approach utilized a set of equations analogous to the Williams–Landel–Ferry equation for melts between the glass-transition temperature (T_g) and T_g + 100 °C, whereas the second approach used equations of the Arrhenius form for melts more than 100 °C above T_g. The combination of these traditional viscoelastic scaling models with predictions for T_g depression by a diluent (Chow model) were used to estimate the observed effects of dissolved CO_2 on polymer melt rheology. In this approach, the only parameters involved are physical properties of the pure polymer melt that are either available in the existing literature or can be measured under atmospheric conditions in the absence of CO_2. The ability of the proposed scaling models to accurately predict the viscosity of polymer melts with dissolved high-pressure CO_2 were examined for each of the polymer systems. © 2001 John Wiley & Sons, Inc. J Polym Sci Part B: Polym Phys 39: 3055–3066, 2001

Keywords: rheology; high pressure; supercritical fluids; viscoelastic scaling

INTRODUCTION

The measurement and modeling of the rheological properties of polymer melts plasticized by high-pressure carbon dioxide (CO_2) or other supercritical fluids (SCFs) is an important tool in assessing the industrial applicability of several novel polymer synthesis and processing applications. Industrial processes requiring such experimental data include gas-assisted injection-molding,[1,2] extrusion,[3] microcellular foaming,[4–6] and melt-phase synthesis reactions.[7] In each of these processes, it is essential to quantify the role of CO_2 or other SCF plasticizers for optimization of both equipment design and end-of-the-line products.

In a set of recent publications, several investigators have presented rheological evidence for the

Correspondence to: S. A. Khan (E-mail: khan@eos.ncsu.edu)

Journal of Polymer Science: Part B: Polymer Physics, Vol. 39, 3055–3066 (2001)
© 2001 John Wiley & Sons, Inc.

plasticization of polymer melts by compressed liquid and supercritical CO_2, $scCO_2$. Specifically, poly(dimethylsiloxane) (PDMS),[8] poly(ethylene glycol) (PEG),[9] poly(methyl methacrylate) (PMMA),[10] and polystyrene (PS)[11–13] have all been investigated at various CO_2 concentrations, temperatures, and pressures. These polymer systems have been chosen because of their wide commercial use in extrusion-based processes in which transient plasticization via CO_2 could be advantageous. In addition to generating rheological data, some investigators have also attempted to develop models that quantify the observed viscosity reduction by dissolved CO_2.[12,14] This has generally been done by constructing rheological master curves that in principle can help to predict the rheological properties of polymer melts plasticized by CO_2. Gerhardt et al.[14] have presented an approach that utilizes a lattice fluid equation of state to predict the free volume of a plasticized melt and coupled it with a modified Kelly and Bueche[15] equation to relate free volume and viscosity. This model worked well for CO_2 plasticization of PDMS, but has not been reported to apply to any other polymeric systems. Lee et al.[12] used a generalized viscoelastic fluid model with eight adjustable parameters to model the CO_2-induced plasticization of PS. Although this model does accurately collapse the experimental data, the adjustable parameters make the universal application and predictability of the model cumbersome.

In a previous study,[13] we presented an approach to predict the viscoelastic scaling of CO_2-plasticized polymer melts that combines a theoretical prediction for the glass-transition temperature (T_g) depression of a polymer by a diluent with a traditional free-volume model for viscoelastic scaling, such as the Williams–Landel–Ferry (WLF) equation.[16] This study expands the scope of our earlier work and presents a modification to our original model to quantify the observed viscosity reduction of polymer melts by dissolved CO_2 using an Arrhenius expression (which is suitable for melts at temperatures 100 °C above T_g) coupled with the prediction of T_g reduction. This approach further exemplifies that coupling of T_g depression with viscoelastic scaling models provides a quantitative and predictive understanding of the effects of pressure, temperature, and CO_2 concentration on the rheology of a plasticized polymer melt.

In this article, the rheological measurements of several polymer melts plasticized by CO_2 are used to illustrate the applicability of the two viscoelastic scaling models: one using a modified WLF equation and a second using a modified Arrhenius expression. Specific experimental data for the viscosity reduction by the addition of CO_2 are given for PMMA, poly(vinylidene fluoride) (PVDF), isotactic polypropylene (iPP), and low-density polyethylene (LDPE). The applicability of our predictive viscoelastic scaling models is addressed for each of these cases. Because the parameters involved in these models only use physical properties of the plasticizer and the undiluted polymer matrix, our method provides a generalized approach for predictively scaling rheological properties of plasticized melts.

VISCOELASTIC SCALING THEORY

T_g Depression

The depression of T_g with the addition of CO_2 and other diluents has been widely reported for many polymer systems.[17–22] Chow[23] proposed the following expression to predict the T_g of polymer diluent mixtures on the basis of both classical and statistical thermodynamics:

$$\ln\left(\frac{T_{g,mix}}{T_g}\right) = \Psi\{(1-\theta)\ln(1-\theta) + \theta \ln \theta\} \quad (1)$$

$$\theta = \frac{M_p}{zM_d}\frac{\omega}{1-\omega} \quad (2)$$

$$\Psi = \frac{zR}{M_p \Delta C_{pT_g}} \quad (3)$$

where $T_{g,mix}$ is the glass-transition temperature of the diluent polymer mixture, ω is the weight fraction of diluent, z is a lattice coordination number for the polymer repeat unit, $\Delta C_{p,T_g}$ is the change in heat capacity associated with the T_g, and M_p and M_d are the molecular weights of the monomer and diluent, respectively. This equation has been shown to be an effective estimate of polymer T_g depression, specifically for PS and PMMA with various diluents including carbon dioxide up to a weight fraction of approximately 12 % at which point the effects of pressure become significant.[23–25] Because this equation was not specifically developed for high pressures, it allows the effects of concentration on T_g to be investigated separately from effects of pressure as long

as the concentration of the dissolved SCF is sufficiently low.

WLF Analogues

We adopt the following expression for the free volume of a polymer melt as a starting point for development of our viscoelastic scaling approach:

$$f = f_g + \alpha\left[T - T_{g,mix} - \frac{\beta}{\alpha}(P - P_0)\right] \quad (4)$$

where f is the free volume of the polymer melt, f_g is the free volume at the T_g, α is the difference in the rate of the free-volume expansion above and below T_g, β is the isothermal compressibility of the polymer melt, and P and P_o refer to the system pressure and atmospheric pressure, respectively. This expression suggests that the effects of CO_2 concentration and pressure can be directly incorporated as shifts in the T_g of the polymer melt. Referencing CO_2 concentrations as a T_g depression and pressure as a T_g increase, both CO_2 concentration and pressure can be manipulated in a similar manner to temperature with respect to viscoelastic scaling.

Using the preceding free-volume expression, viscoelastic scaling relationships similar to the WLF model for temperature are obtained. The resulting viscoelastic scaling relationships are presented in eqs 5 and 6; a detailed derivation for these equations is found in a previous article[13]

$$\log(a_p) = \log\left(\frac{\eta_{T,P,c}}{\eta_{T_{g,mix},P,c}} \cdot \frac{\eta_{T_{g,mix},P_0,c}}{\eta_{T,P_0,c}}\right) = \log\left(\frac{\eta_{T,P,c}}{\eta_{T,P_0,c}}\right)$$
$$= \frac{c_1(T - T_{g,mix,P_0})}{c_2 + T - T_{g,mix,P_0}} - \frac{c_1(T - T_{g,mix,P})}{c_2 + T - T_{g,mix,P}} \quad (5)$$

$$\log(a_c) = \log\left(\frac{\eta_{T,P_0,c_0}}{\eta_{T_{g,mix},P_0,c_0}} \cdot \frac{\eta_{T_g,P_0,c}}{\eta_{T,P_0,c}}\right) = \log\left(\frac{\eta_{T,P_0,c_0}}{\eta_{T,P_0,c}}\right)$$
$$= \frac{c_1(T - T_{g,P_0})}{c_2 + T - T_{g,P_0}} - \frac{c_1(T - T_{g,mix,P_0})}{c_2 + T - T_{g,mix,P_0}} \quad (6)$$

where c_1 and c_2 are the WLF constants, the subscripts P and P_o refer to the viscosity data at a given pressure P and that corrected to atmospheric pressure, and c and c_o refer to the data with CO_2 and corrected to a CO_2 concentration of zero. a_P and a_C correspond to the shift factors associated with pressure and concentration, respectively. These shift factors, in conjunction with the traditional time-temperature superposition factor a_T, can be used collectively to scale viscosity under different experimental conditions.

Arrhenius Analogues

The aforementioned WLF analogues (eqs 5 and 6) are valid only for a polymeric system that can be shifted to a single master curve for temperature using the WLF equation. The WLF equation is generally applicable at temperatures between T_g and T_g + 100 °C, where the increase in free volume with temperature is linear. Above this temperature range, the dependence of viscosity is often described by an Arrhenius expression as follows[27]

$$\ln a_T = \ln\left(\frac{\eta_T}{\eta_{T_0}}\right) = \left[\frac{E_a}{R}\left(\frac{1}{T} - \frac{1}{T_0}\right)\right] \quad (7)$$

where E_a is known as the activation energy for viscous flow, and T_o is an arbitrary reference temperature. In cases where the WLF analogues are not applicable or the standard WLF equation for time-temperature superposition does not shift the experimental data, incorporation of concentration and pressure-dependent terms in the Arrhenius expression would be extremely useful in predicting viscoelastic properties of plasticized polymer melts. To include pressure and concentration corrections, the same method used to develop the WLF analogues is applied.[13] Both concentration and pressure are referenced as shifts in T_g, and then a set of composite viscoelastic scaling relationships are developed. Substitution of these corrections for concentration and pressure result in the following analogues to the original Arrhenius expression to collapse the experimental viscosity data for the CO_2/polymer mixture elevated well above T_g to a single master curve:

$$\ln a_P = \ln\left(\frac{\eta_{T_{g,P_0,mix}}}{\eta_{T_{g,P,mix}}}\right) = \left[\frac{E_a}{R}\left(\frac{1}{T_{g,P_0,mix}} - \frac{1}{T_{g,P,mix}}\right)\right] \quad (8)$$

$$\ln a_C = \ln\left(\frac{\eta_{T_{g,P_0,mix}}}{\eta_{T_{g,P_0}}}\right) = \left[\frac{E_a}{R}\left(\frac{1}{T_{g,P_0}} - \frac{1}{T_{g,P_0,mix}}\right)\right] \quad (9)$$

The value of E_a can be obtained from viscosity measurements of the undiluted polymer melt. Therefore, these equations as with the WLF analogues provide predictive scaling for the effects of pressure and diluent concentration, requiring

Table I. Charaterization of Polymeric Samples

Polymer	M_n	M_w	PDI
PMMA-VO45	90,700	140,600	1.55
PMMA-VM100	69,700	106,700	1.53
LDPE	21,987	72,477	3.30
PP-4036	33,437	204,745	6.12
PP-4018	28,838	132,881	4.61
PVDF-Kynar 740	100,100	156,000	1.56
PVDF-Kynar 460	260,500	534,000	2.05

only the rheological properties of the neat polymer melt to be directly measured.

EXPERIMENTAL MATERIALS AND METHODS

Materials

Several commercially available polymeric samples were used for this study. Two PMMA samples, VO45 and VM100, were procured from AtoHaas Americas Inc. (King of Prussia, PA). Two isotactic polypropylene samples, PP-4036 and PP-4018, were obtained from BP Amoco (Naperville, IL). Additionally, LDPE 640I was acquired from Dow Chemical (Midland, MI). Finally, two poly(vinylidene fluoride) samples, Kynar 740 and Kynar 460, were obtained from Elf Atochem (King of Prussia, PA). All samples were obtained in pellet form and used as received. Rheological experiments were performed using a single batch of each polymer resin to ensure uniformity. Liquid carbon dioxide (bone dry grade 2.8; purity >99.8%) was obtained from National Welders and used as received.

Table I summarizes the molecular weight and molecular weight distribution information for each of the polymer samples used. Several different techniques were used to determine this information. The two PMMA samples (VO45 and VM100) were dissolved in tetrahydrofuran, and molecular weight information was determined by gel permeation chromatography (GPC). The PMMA samples were measured relative to PS standards, and the appropriate Mark–Houwink parameters were used to calculate the actual PMMA molecular weights. The LDPE and PP samples were measured using a high-temperature GPC with a calibration curve developed for PS standards dissolved in 1,2,4-trichlorobenzene. The molecular weights were obtained from the universal calibration curve using the appropriate Mark–Houwink constants. Finally, the molecular weight information for both of the PVDF samples were provided by the manufacturer.

Rheometer and Experimental Procedure

The experimental apparatus used in our study is based on the extrusion rheometers developed first by Han and Ma.[28–30] The specifics of our rheometer design can be found elsewhere.[13] Basically, an adapter, a slit die, and a nozzle are attached to the outlet of the extruder. The adapter (Wayne Machine and Die) is required to connect the slit die to the face of the extruder barrel. A static mixer (Omega FMX8441S) is inserted into the adapter to enhance mixing and aid in the formation of a one-phase mixture prior to the slit die. Two slit dies were designed to allow for a large range of viscosities to be measured. The nozzle is required to elevate the pressure within the slit die above the bubble pressure ensuring that a one-phase mixture is maintained during measurement with CO_2. The pressure drop and temperature across the slit die were measured via three melt transducers (Dynisco TPT432A-7.5M-6/18).

The viscosity of a polymer melt can be calculated using the following equations:[31–33]

$$\text{Shear stress} \qquad \tau_w = \left(\frac{-\Delta P}{L}\right)\frac{H}{2} \tag{10}$$

$$\text{Apparent shear rate} \qquad \dot{\gamma} = \left(\frac{6Q}{WH^2}\right) \tag{11}$$

$$\text{Apparent viscosity} \qquad \eta_{app} = \frac{\sigma_w}{\dot{\gamma}_{app}} \tag{12}$$

where L is the length of the die, W is the slit width, H is the slit height, Q is the volumetric flow rate, and ΔP is the pressure drop. To obtain viscosity measurements at constant CO_2 concentrations, calibration of the mass flow rate is required. Equations 10–12 are strictly valid for fully developed flows of incompressible fluids; the effects of pressure on the compressibility of the fluids used here are discussed subsequently, and these equations are valid. To accomplish this calibration, the polymer sample is fed to the extruder via the hopper, and the extruder screw is used to generate pressure, forcing the melt into the slit die. The pressure drop is recorded, and samples of the melt are taken at the exit of the die to measure the mass flow rate. The volumetric flow rate that is required to determine the viscos-

Table II. Characteristic Sanchez–Lacombe Parameters

Material	ρ^* (g/cm^3)	T^* (K)	P^* (MPa)	Reference
PMMA	1.281	668	516.9	47
PP	0.938	570	354.2	47
LDPE	0.919	610	421.4	47
PVDF	1.105	735	357	47
Carbon dioxide	1.426	328.1	464.2	48

ity of the melt is calculated using the measured mass flow rate and the density estimated from an equation of state. For the purpose of this analysis, the Sanchez–Lacombe equation of state[34–36] is used with the mixing rules described previously (no interaction parameter is used).[37] A list of the Sanchez–Lacombe parameters used for all of the polymer samples and CO_2 are found in Table II. The procedure is repeated at different screw rotation rates to develop a viscosity curve and mass flow-rate calibration as a function of shear rate for the neat polymer.[13]

To ensure that both fully developed flow along with a single-phase mixture is present during measurement, the pressure profile as a function of die length needs to be examined. It has been noted previously[13] that in the absence of CO_2 the pressure drop as a function of length must be linear to ensure the flow within the die is fully developed and free of entrance effects. When compressed CO_2 is dissolved in the melt, the linear pressure drop takes on additional significance. If the pressure profile as a function of length is nonlinear in the presence of CO_2, this is a signature of a two-phase mixture. In the presence of a separate CO_2 phase, the apparent viscosity of the polymer will increase both because of the lower concentration of CO_2 dissolved in the matrix and the surface energy associated with the deformation of bubble.[33] All systems presented in this work were run under conditions of a linear pressure drop within the measurement region of the slit die to ensure that a single-phase fully developed flow was present. It should be pointed out that prior to establishment of steady-state pressures in the slit die and during increases in CO_2 concentration, two-phase flow was observed. This can be sharply contrasted from the conditions of single-phase flow described previously. When two-phase flow occurs, large pressure fluctuations (10 MPa) are observed in the die, and the extrudate is highly nonuniform with large pockets of undissolved CO_2. During our measurements, the fluctuations in pressure were less than 0.1 MPa, the extrudate was uniform, and the flow rate was constant over long ranges of time (10–15 min).

The viscosity of the plasticized melt with dissolved CO_2 is measured using a procedure similar to that for the neat melt. The desired amount of CO_2, based on the polymer mass flow-rate calibration, which was found to be independent of CO_2 concentration, is injected by varying the tension on the back pressure relief valve and the flow rate of the syringe pump. A minimum of 5 min is allowed at each flow rate after the system has reached steady state. Steady state is attained when the pressure of both the injection system and slit die has stabilized after a change in either the CO_2 injection rate or screw-rotation rate. The CO_2 polymer-solution density is calculated using the Sanchez–Lacombe equation of state. The values obtained for the mixture density correspond well with experimental solubility measurements found in the literature.[11,25,38] The pressure drop across the die and the volumetric flow rate of the mixture are used to determine the apparent viscosity as a function of shear rate using eqs 10–12.

Mixture Compressibility

Because our method to measure viscosity involves a pressure-driven Poiseuille flow, it is necessary to clarify issues associated with the pressure gradient generated along the length of the die. The most important parameter to examine in this case is the compressibility of the polymer and polymer/CO_2 mixtures. Using the Sanchez–Lacombe equation of state, Table III has been constructed to better explain the effects of pressure on the density of the pure polymer and polymer/CO_2 mix-

Table III. Comparison of Pure Polymer and Polymer/CO_2 Mixture Compressibility for PVDF at 250 °C

CO_2 Content (wt %)	Pressure (MPa)	Density (g/cm^3)	Density Change (%)
0	19.5	1.37	—
0	3.0	1.33	2.2
2	19.5	1.34	—
2	3.0	1.30	2.9
4	19.5	1.32	—
4	3.0	1.27	3.7

tures. PVDF has been chosen as a representative polymer, and the other polymers used in this work, specifically PMMA, PP, and LDPE, follow very similar patterns of behavior. By examining the first two rows of the table, as the pressure is changed from 19.5 MPa (an average value for the pressure at the die entrance) to 3.0 MPa (an average pressure value for the die exit), the density of the pure polymer (no CO_2) changes from 1.37 to 1.33 g/cm^3 at 250 °C. This change in density is approximately a 2.2% change in the density of the polymer. This method for viscometric measurement of polymer systems is a well accepted measurement technique, and the effects of this small change in compressibility are generally accepted to be insignificant when compared with the sensitivity of the pressure transducers.[27,33,39–43] When the same range of pressures at 250 °C are examined for a CO_2 concentration of 2 and 4 wt % the changes in density are 2.9 and 3.7%, respectively. This added ~1% compressibility of the polymer/CO_2 mixture in comparison to the pure polymer melt is once again considered to be insignificant when compared with the errors in transducer sensitivity. This assumption has been used by several other researchers and shown to be adequate for this type of mixture, therefore justifying the use of eqs 10–12.[8,9,11,13,14,28–30] However, it is important to note that the experiments conducted in this work are at low concentrations of CO_2 with a polymer melt. This assumed incompressibility of the mixture will not be valid over the entire range of mixture concentrations and can produce significant errors at larger CO_2 concentrations.

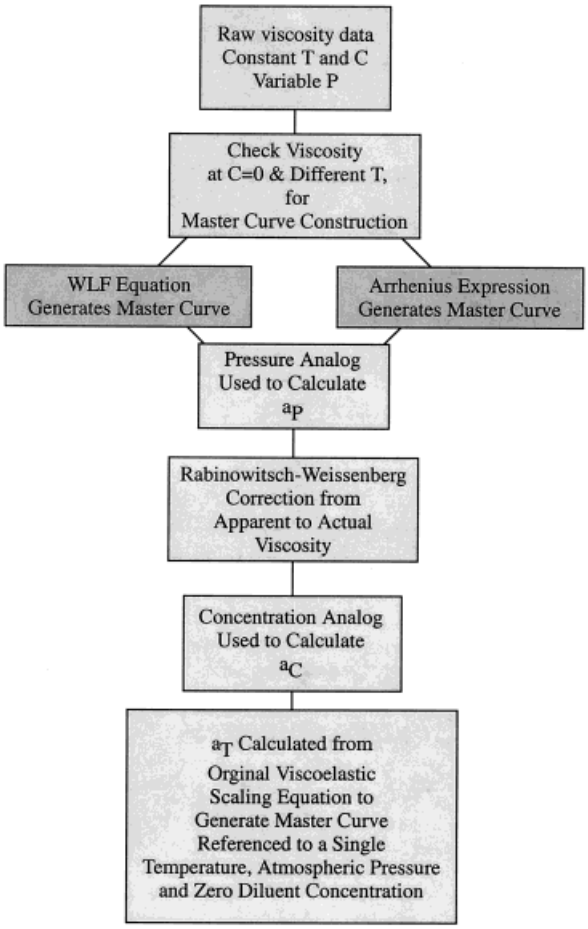

Figure 1. Outline of steps required to construct a viscosity master curve using either of the two viscoelastic scaling analogues.

Viscoelastic Scaling Procedure

Shifting of the experimental viscosity data is accomplished by following a four-step process. Figure 1 provides a simple outline of the required shifting procedure. Initially an applicable model, either the WLF or the Arrhenius analogues, must be tested to ensure that the model accurately describes the rheological data of the unplasticized polymer matrix. Once a model has been chosen, all experimental viscosity measurements can be grouped into data sets consisting of points at constant temperature and constant concentration as a function of shear rate. However, all points in each of the sets are taken at different average pressures. The first step in the viscoelastic shifting procedure is to correct all experimental measurements to a common reference pressure, P_o, using either eq 5 or 8 depending on the applicable model. The isothermal compressibility, β, required for the pressure correction, is determined from published PVT data of similar commercial resins.[44] The PVT data of a pure polymer system is used so that the effects of pressure and CO_2 concentration can be isolated. After shifting of the data for pressure, the Rabinowitsch–Weissenberg correction can be used to correct the measurements from apparent viscosity to actual viscosity.[41] Finally, the corrections for concentration (eqs 6 or 9) and temperature (WLF equation or eq 7) can be used to obtain a master curve. All parameters used for the viscoelastic scaling of the melt with dissolved CO_2 can either be directly measured or calculated from the unplasticized polymer melt and pure CO_2. The only true adjustable parameter for the effects of pressure and CO_2 concentration is the choice of the lattice coordinate parameter, z. The lattice coordinate param-

eter, z, is the thermodynamic parameter that distinguishes the number of lattice spaces a monomeric unit occupies in the thermodynamic model in comparison to that of a CO_2 molecule. In the case of PMMA, experimental T_g depression data are available in the existing literature,[24] and therefore z was determined from the best fit of Chow's T_g depression model to the experimental data. In all other cases, z was estimated as the nearest whole number to the ratio of the molecular size of the monomer relative to CO_2.

RESULTS AND DISCUSSION

Poly(methyl methacrylate) (PMMA)

Experimental measurements of viscosity reduction for two commercial PMMA samples at 210 °C with the addition of pressurized CO_2 are displayed in Figure 2. In Figure 2(a), the viscosity of the PMMA V045 system is shown at concentrations of 4 and 6 wt % CO_2, whereas Figure 2(b) displays the PMMA VM100 viscosity with dissolved CO_2 concentrations of 2, 3, and 4 wt %. The average pressures, in megapascals, attained within the slit die are given for the experimental measurements in Figure 2(a) as a representative sample of the experimental conditions for PMMA and the other polymer discussed herein. To obtain more detailed information concerning the exact pressures of these experiments, interested readers are asked to consult extensive data tables published elsewhere.[45,46] From these data, it is clear that the incorporation of CO_2 into the polymer melt significantly reduces the viscosity of the polymer matrix for both PMMA systems. For example, the PMMA V0-45 sample with 6 wt % CO_2 shows almost an 80% reduction in viscosity at a shear rate of 10 s^{-1}. These data are consistent with similar observed viscosity reductions on the PMMA/CO_2 system available in the literature.[10]

The T_g of both PMMA samples was found to be 100 °C as measured by DSC. Although the WLF region is generally applicable to 100 °C above T_g, experimental curve fitting of the undiluted polymer melt as a function of temperature confirms that the WLF equation does collapse the experimental data to a master curve up to approximately 150 °C above T_g. Thus, the WLF analogues are used to collapse the CO_2/PMMA viscosity data found in Figure 2 to a single master curve for each polymeric sample. The results of the viscoelastic scaling for PMMA are shown in Figure 3,

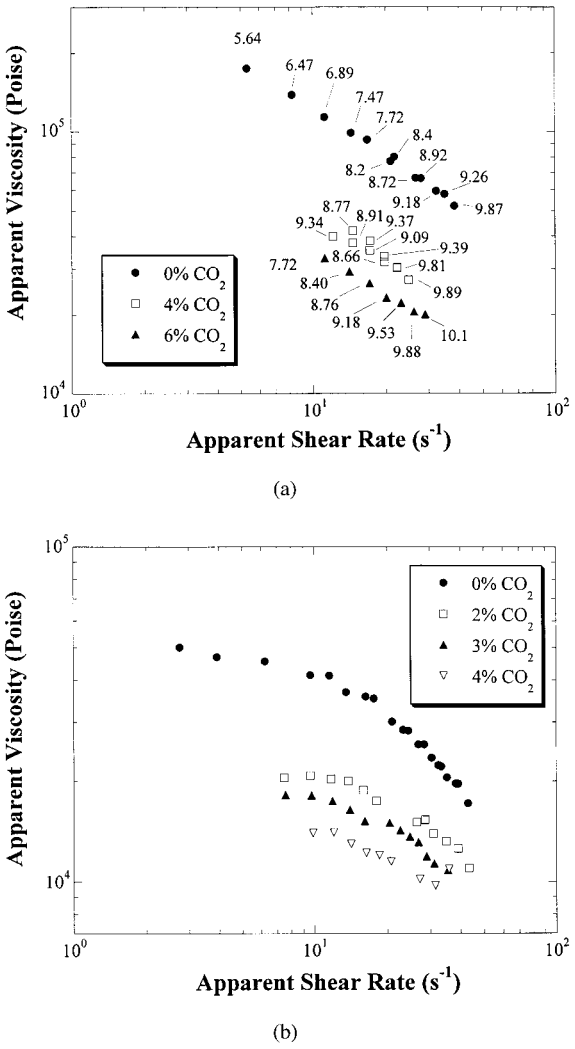

Figure 2. Viscosity versus shear-rate behavior of PMMA at various concentrations of dissolved carbon dioxide at 210 °C for two different samples: (a) VO45 and (b) VM100. The average pressures (MPa) in the slit die during measurement are provided as a representative sample in (a).

and the parameters used in the shifting procedure are contained in Table IV. In Figure 3, the WLF analogues overlay the data onto a single curve for each of the two polymer resins. The error in the master-curve construction is less than 5%, which is on the order of magnitude of error previously determined for the experimental device.[13] Therefore, within the accuracy of the experimental apparatus, the WLF analogue for pressure and concentration accurately represents the experimentally observed viscosity reduction. Detailed rheological data for the PMMA/CO_2 system as well as the other polymer systems inves-

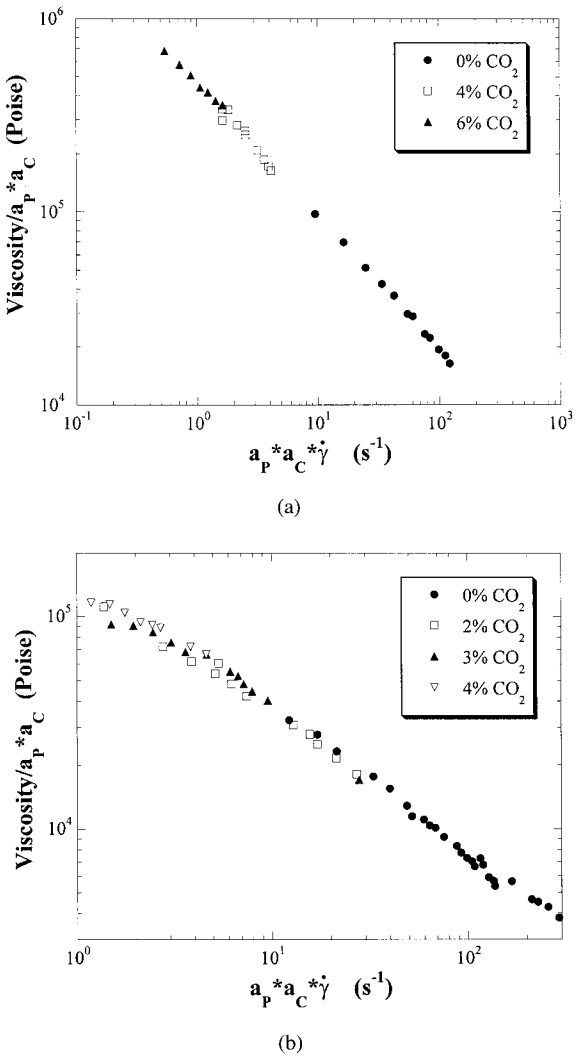

Figure 3. Viscosity master curves generated using the WLF scaling analogues. Each curve is collapsed at 210 °C, atmospheric pressure, and zero carbon dioxide concentrations: (a) VO45 resin and (b) VM100 resin.

tigated in this article are found elsewhere.[46] It is important to reiterate that the viscoelastic master curves shown here from PMMA and in the following section are all constructed using the theoretical predictions of T_g depression and elevation and are not a result of calculating a best fit set of shift factors. We believe that our approach

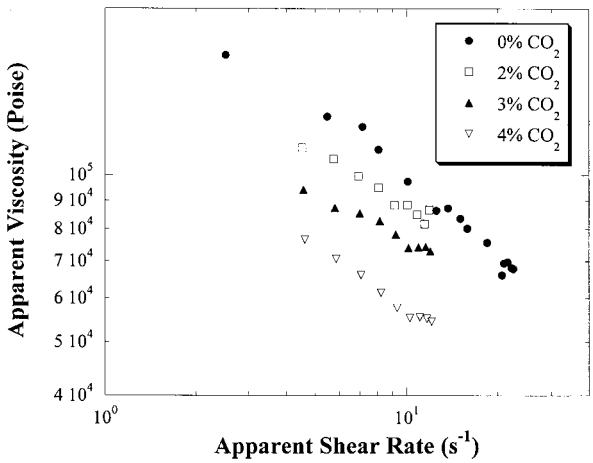

Figure 4. Viscosity versus shear-rate behavior of polypropylene, PP-4018, at various concentrations of dissolved carbon dioxide and 190 °C.

therefore provides a more solid understanding of CO_2 induced plasticization as compared to earlier viscoelastic scaling models.

Polypropylene (PP)

Viscosity measurements for the two different commercial iPP polymers over a range of temperatures and CO_2 concentrations were measured using the extrusion slit die rheometer. A representative set of experimental results for the PP-4018 sample at 190 °C at various CO_2 concentrations is depicted in Figure 4. Once again, large reductions in the melt viscosity with the addition of CO_2 are observed. Specifically for the PP-4018 sample, almost 50% reduction in viscosity with 4 wt % CO_2 is measured at 190 °C.

The T_g of both iPP samples was found to be −10 °C by DSC experiments. Examination of the rheological measurements of the pure polymer melt (no CO_2) at various temperatures suggested that an Arrhenius expression with a fitted activation energy of 4.27×10^4 (J/mol) accurately describes the rheological behavior as opposed to the WLF equation.[27] Using the Arrhenius analogues for concentration and pressure, master curves for

Table IV. WLF Analogue Scaling Model Parameters

Polymer	M_p	ΔC_p (J/g · mol)	c_1	c_2	T_g (K)	z	β (1/MPa)	α (1/K)
PMMA	100	32.7	17.44	51.6	378	4	$6.5 \cdot 10^{-4}$	$4.8 \cdot 10^{-4}$

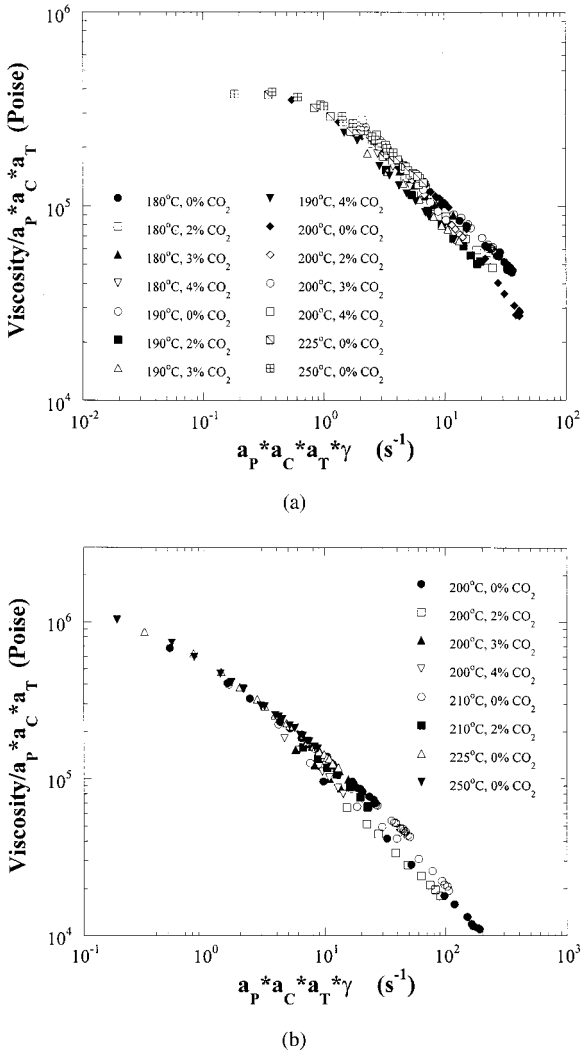

Figure 5. Viscosity master curves generated using the Arrhenius scaling analogues. Each curve is collapsed to a single temperature, atmospheric pressure, and zero carbon dioxide concentrations: (a) PP-4018 at 180 °C and (b) PP-4036 at 200 °C.

each of the two iPP samples are constructed and shown in Figure 5. Similar errors in the master curves constructed for PP in comparison with the PMMA results are observed. The shifting constants used for the viscoelastic scaling of PP are displayed in Table V. This system shows that the Arrhenius expression for temperature coupled with the appropriate model for the effects of pressure and CO_2 concentration on T_g quantitatively captures the rheological behavior of the melt plasticized by pressurized CO_2.

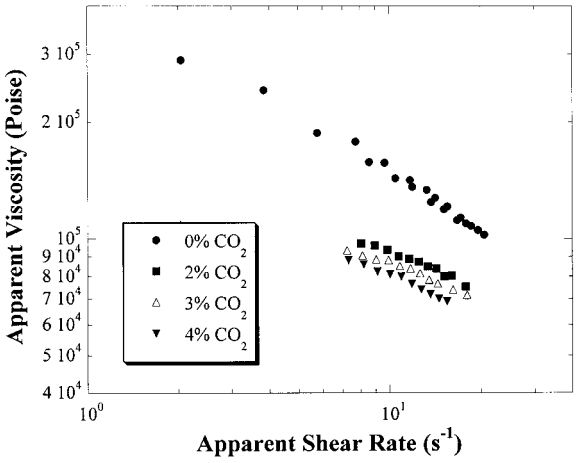

Figure 6. Apparent viscosity measurements of LDPE 640I at various concentrations of dissolved carbon dioxide and 200 °C.

Low-Density Polyethylene (LDPE)

Rheological measurements for the LDPE sample at 200 °C and various concentrations of compressed CO_2 are shown in Figure 6. As with the other polymeric melts, CO_2 acts as an extremely effective plasticizer for LDPE. In this case, for a CO_2 concentration of 4 wt % at a shear rate of 10 s^{-1}, a viscosity reduction of nearly 75% in comparison with the unplasticized melt is realized.

To correlate the viscosity reduction of the LDPE sample, the Arrhenius equation approach is deemed appropriate because the WLF model does not capture the thermorheological behavior of the unplasticized melt in this temperature regime (nearly 300 °C above T_g). Experimental

Table V. Arrhenius Analogue Scaling Model Parameters

Polymer	M_p	ΔC_p (J/g · mol)	E_a (J/mol)	T_g (K)	z	β (1/MPa)	α (1/K)
PP	42	19.2	$4.27 \cdot 10^4$	263	1	$1.15 \cdot 10^{-3}$	$4.8 \cdot 10^{-4}$
LDPE	28	10.5	$5.53 \cdot 10^4$	237	1	$1 \cdot 10^{-3}$	$4.8 \cdot 10^{-4}$
PVDF	64	21.2	$8.34 \cdot 10^4$	212	1	$8.2 \cdot 10^{-3}$	$4.8 \cdot 10^{-4}$

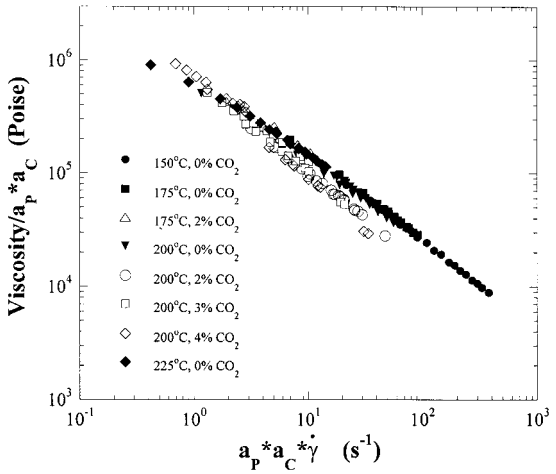

Figure 7. LDPE viscosity master curves generated using the Arrhenius scaling analogues collapsed to 200 °C, atmospheric pressure, and zero concentrations.

measurements of pure LDPE for various temperatures ranging between 150 and 200 °C could be fitted to the Arrhenius expression accurately yielding a value of 5.53×10^4 J/mol for the activation energy, E_a. This value of E_a together with other known constants for the pure melt collapse all data for the LDPE systems with varying amounts of CO_2 to a single master curve, as seen in Figure 7. As with PP, the Arrhenius analogues for viscoelastic scaling predict the CO_2 viscosity reduction of the LDPE melt to within 5%, or is on the order of magnitude of the experimental error. All of the shifting parameters used to shift the viscosity data of LDPE with the Arrhenius analogs for pressure and concentration are listed in Table V.

Poly(vinylidene fluoride) (PVDF)

A representative set of rheological measurements is shown for PVDF at several different CO_2 concentrations in Figure 8. As with the other systems a detailed collection of experimental data for each of the two PVDF at several temperatures can be found elsewhere.[46] In the case of PVDF, the solubility of CO_2 in the molten polymer melt is lower than the other polymer samples measured under similar conditions. Solubility limits in this case are determined by the detection of two-phase flow during viscosity measurements. If the pressure drop in the slit die becomes nonlinear, two-phase flow (or CO_2/polymer-phase separation) is assumed to occur. This low solubility limits the maximum CO_2 concentration that can be maintained as a one-phase system during rheological measurement to 2 or 3 wt %, depending on the temperature. Typically, a 40% viscosity reduction is observed with the addition of 2 wt % CO_2 at each of the temperatures measured.

The viscosity measurements in this article were taken at temperatures nearly 300 °C above the T_g of PVDF, which is approximately −61 °C. The WLF model does not accurately account for the viscoelastic scaling with temperature in the absence of CO_2, and therefore the Arrhenius analogues for viscoelastic scaling are used. The value for E_a is again fitted to the experimental temperature data of the unplasticized polymer melt and is 8.34×10^4 J/mol. All of the values required for the shifting of PVDF using the Arrhenius scaling analogues are displayed in Table V. The master curves generated using this viscoelastic scaling for each of the two resins are shown in Figure 9. The master curve generated for the Kynar 460 sample, Figure 9(a), collapses the experimental data within the error of 5%, and the master curve for the Kynar 740 system [Fig. 9(b)] exhibits a similar level of error.

Applicability of Scaling Procedure

In determining the applicability of this viscoelastic scaling approach to other polymeric systems, one needs to consider several issues. First, as previously discussed, the diluent/polymer mixture needs to exhibit compressibilities along the same order of magnitude as the pure polymer. This will ensure that the equations used to calcu-

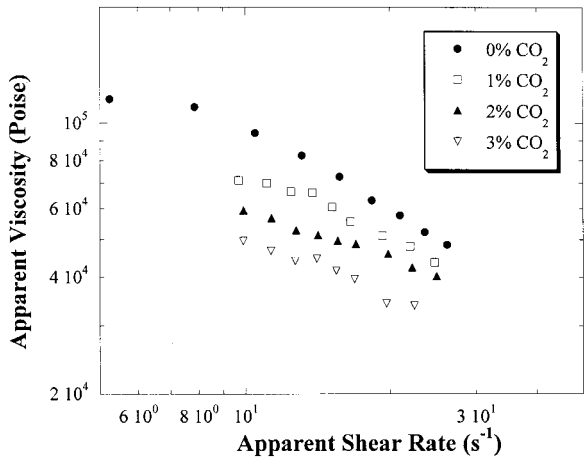

Figure 8. Apparent viscosity measurements of PVDF-Kynar 740 at various concentrations of dissolved carbon dioxide and 210 °C.

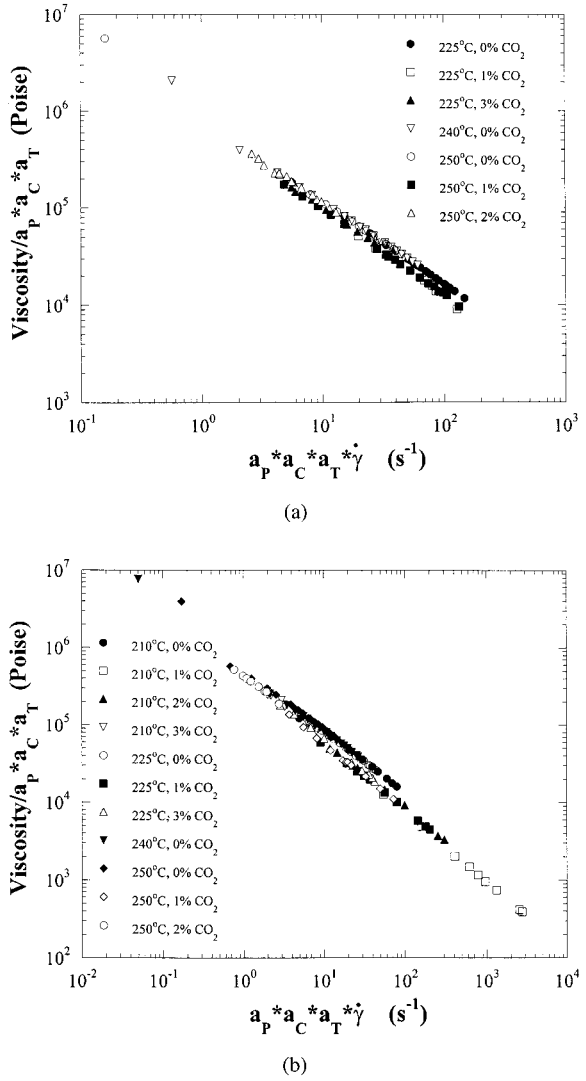

Figure 9. Master curves generated using the Arrhenius scaling analogues. Each curve is collapsed to a single temperature, atmospheric pressure, and zero concentrations: (a) Kynar 460 at 225 °C and (b) Kynar 740 at 210 °C.

late both the viscosity and the shear rate are valid. Second, the prediction of T_g shifts with both pressure and concentration must accurately model the physical behavior of the system. Although the success of our method in collapsing the rheological data to a single master curve for each of the polymer samples studied suggests that the Chow model is accurately capturing the T_g depression behavior for the polymers, the applicability of the Chow model may not be universal. Even if the Chow model fails for some polymers, our approach provides a general framework to couple other T_g depression models with viscoelastic models to decipher the effects of concentration, pressure, and temperature on polymer melt viscosity.

CONCLUSIONS

In this study, existing theories for viscoelastic scaling of polymer melts (WLF and Arrhenius models) combined with the prediction of T_g depression by a diluent (Chow model) were used to predict the observed effects of dissolved CO_2 on polymer melt rheology. The free-volume models depend only on material parameters of the pure polymer melt that are available in the existing literature for most polymers or can be easily measured from the polymer under atmospheric conditions in the absence of CO_2.

Measurements of CO_2/polymer mixture viscosities for several different polymer melts were used to probe the general applicability of the two viscoelastic scaling models. Classical viscoelastic scaling was performed using the predictive free-volume models to collapse each of the experimental data sets to a single master curve independent of pressure and CO_2 concentration for the polymer resins. The rheological data for both PMMA samples collapsed to a single master curve using the WLF analogue, whereas the rheological data for the PP systems, the LDPE, and both of the PVDF samples were collapsed a single master curve using the Arrhenius analogues. Because the data for these polymer/CO_2 systems collapse to master curves using the Arrhenius and WLF analogues expression, we believe that this validates the Chow model for T_g depression for systems that have not been experimentally measured such as PP, LDPE, and PVDF.

The experimental data reveal that the predictive viscoelastic scaling models can be applied to a variety of polymer resins over a wide range of temperatures at low concentrations of CO_2 (where the Chow model appears to be valid). The use of these models should not only be constrained to CO_2 but quantitatively explain the effects of other diluents on the rheology of a polymer melt.

This material is based on work supported in part by the STC Program of the National Science Foundation under Agreement CHE-9876674. Additional funding was also provided by the Kenan Center for the Utilization of Carbon Dioxide in Manufacturing at North Carolina State University and the University of North Carolina

at Chapel Hill. The authors thank Y. Gay for his experimental work on portions of this project, Dr. S. Gross for the DSC measurements, and S. Folk and Dr. K. Huchenson (DuPont) for the GPC analysis.

REFERENCES AND NOTES

1. Chao, S. M.; Wang, S. M.; Chen, S. C. Polym Eng Sci 2000, 40, 583–594.
2. Wang, D. Y.; Wang, J.; Qu, X. Z.; Liang, R. F.; Qi, Z. N. Acta Polym Sinica 2000, 1, 111–113.
3. Huang, Q.; Seibig, B.; Paul, D. J Membr Sci 1999, 161, 287–291.
4. Kraynik, A. M. Polym Eng Sci 1981, 21, 80–85.
5. Park, C. B.; Behravesh, A. H.; Venter, R. D. Polym Eng Sci 1998, 38, 1812–1823.
6. Doroudiani, S.; Park, C. B.; Kortschot, M. T. Polym Eng Sci 1998, 38, 1205–1215.
7. Gross, S. M.; Givens, R. D.; Jikei, M.; Royer, J. R.; Khan, S. A.; DeSimone, J. M.; Odell, P. G.; Hamer, G. K. Macromolecules 1998, 31, 9090–9092.
8. Gerhardt, L. J.; Manke, C. W.; Gulari, E. J Polym Sci Part B: Polym Phys 1997, 35, 523–534.
9. Bae, Y. C.; Gulari, E. J Appl Polym Sci 1997, 63, 459–466.
10. Elkovitch, M. D.; Tomasko, D. L.; Lee, L. J. Polym Eng Sci 1999, 39, 2075–2084.
11. Kwag, C.; Manke, C. W.; Gulari, E. J Polym Sci Part B: Polym Phys 1999, 37, 2771–2781.
12. Lee, M.; Park, C. B.; Tzoganakis, C. Polym Eng Sci 1999, 39, 99–109.
13. Royer, J. R.; Gay, Y. J.; DeSimone, J. M.; Khan, S. A. J Polym Sci Part B: Polym Phys 2000, 38, 3168–3180.
14. Gerhardt, L. J.; Garg, A.; Manke, C. W.; Gulari, E. J Polym Sci Part B: Polym Phys 1998, 36, 1911–1918.
15. Kelley, F. N.; Bueche, F. J Polym Sci 1961, 50, 549.
16. Williams, M. L.; Landel, R. F.; Ferry, J. D. JACS 1955, 77, 3701–3707.
17. Condo, P. D.; Paul, D. R.; Johnston, K. P. Macromolecules 1994, 27, 365–371.
18. Condo, P. D.; Sanchez, I. C.; Panayiotou, C. G.; Johnston, K. P. Macromolecules 1992, 25, 6119–6127.
19. Goel, S. K.; Beckman, E. J. Polymer 1993, 34, 1410–1417.
20. Wissinger, R. G.; Paulaitis, M. E. J Polym Sci Part B: Polym Phys 1991, 29, 631–633.
21. Zhang, Z.; Handa, Y. P. J Polym Sci Part B: Polym Phys 1998, 36, 977–982.
22. Wang, W. V.; Kramer, E. J.; Sachse, W. H. J Polym Sci Polym Phys Ed 1982, 20, 1371–1384.
23. Chow, T. S. Macromolecules 1980, 13, 362–364.
24. Chiou, J. S.; Barlow, J. W.; Paul, D. R. J Appl Polym Sci 1985, 30.
25. Wissinger, R. G.; Paulaitis, M. E. J Polym Sci Part B: Polym Phys 1987, 25, 2497–2510.
26. Fillers, R. W.; Tschoegl, N. W. Trans Soc Rheol 1977, 21, 51–100.
27. Bird, R. B.; Armstrong, R. C.; Hassager, O. Dynamics of Polymer Liquids. In Fluid Mechanics; Wiley-Interscience: New York, 1987; Vol. I, pp 99–163.
28. Ma, C.-Y.; Han, C. D. J Cell Plast 1982, 361–370.
29. Han, C. D.; Ma, C. J Appl Polym Sci 1983, 28, 831–850.
30. Han, C. D.; Ma, C.-Y. J Appl Polym Sci 1983, 28, 851–860.
31. Wales, J. L. S.; denOtter, J. L.; Janeschitz-Kriegl, H. Rheol Acta 1965, 4, 146.
32. Eswaran, R.; Janeschitz-Kriegl, H.; Schijif, J. Rheol Acta 1963, 3, 83.
33. Macosko, C. W. Rheology: Principles, Measurements and Applications; VCH: New York, 1994, pp 237–280.
34. Lacombe, R. H.; Sanchez, I. C. J Phys Chem 1976, 80, 2568–2580.
35. Sanchez, I. C.; Lacombe, R. H. J Phys Chem 1976, 80, 2352–2362.
36. Sanchez, I. C. Macromolecules 1978, 11, 1145–1156.
37. Royer, J. R.; DeSimone, J. M.; Khan, S. A. Macromolecules 1999, 32, 8965–8973.
38. Wissinger, R. G.; Paulaitis, M. E. Ind Eng Chem Res 1991, 30, 842–851.
39. Dealy, J. M.; Wissbrun, K. F. Melt Rheology and Its Role in Plastics Processing; Van Nostrand Reinhold: New York, 1989.
40. Gendron, R.; Correa, A. Cell Polym 1998, 17, 93–113.
41. Laun, H. M. Rheol Acta 1983, 22, 171–185.
42. Padmanabhan, M.; Battacharya, M. Rheol Acta 1994, 33, 71–87.
43. Rauwendaal, C.; Fernandez, F. Polym Eng Sci 1985, 25, 765–771.
44. Zoller, P.; Walsh, D. J. Standard Pressure-Volume-Temperature Data for Polymers; Technomic: Lancaster, PA, 1995.
45. Royer, J. R. http://www.lib.ncsu.edu/etd: Electronic Thesis, 2000.
46. Royer, J. R. Ph.D. Thesis, North Carolina State University, Raleigh, 2000.
47. Polymer Handbook; Bandrup, J.; Immergut, E. H.; Grulke, E. A., Eds.; Wiley: New York, 1999; VI/591–601.
48. Garg, A.; Gulari, E.; Manke, C. W. Macromolecules 1994, 27, 5643–5653.